

# ORIENTATIONAL MELTING OF TWO-SHELL CARBON NANOPARTICLES: MOLECULAR DYNAMICS STUDY.

*Yu. E. Lozovik\*, A. M. Popov*

*Institute of Spectroscopy, Russian Academy of Science, 142190,  
Troitsk, Moscow region, Russia*

The energetic characteristics of two-shell carbon nanoparticles ("onions") with different shapes of second shell are calculated. The barriers of relative rotation of shells are found to be surprisingly small; therefore, free relative rotation of shells can take place at room temperature. The intershell orientational melting of the nanoparticle  $C_{60}@C_{240}$  is studied by molecular dynamics. The parameters of Arrhenius formula for jump rotational intershell diffusion are calculated. The definition of orientational melting temperature is proposed as the temperature when the transition probability over barrier between equivalent potential minima is equal to 1/2. The temperature of orientational melting of the nanoparticle  $C_{60}@C_{240}$  is about 60 K.

## I. INTRODUCTION

The discovery of fullerenes [1] and the elaboration on method of their production in arc discharge [2] give rise to interest in another carbon nanostructures produced in arc discharge, in particular, nanoparticles with shell structure [3,4]. A set of works is devoted to studying their structure and energetics [5]–[13]. Nevertheless, attention has not yet been given to thermodynamical properties of carbon nanoparticles with shell structure.

The melting of a single cluster can differ essentially from phase transitions in macroscopic systems [14]–[22]. Particularly, the melting of a mesoscopic cluster with shell structure can manifest itself as a hierarchy of rearrangements with breaking intershell orientational order and then breaking shell structure and order in particles positions inside shells. For example, in 2D mesoscopic clusters with Coulomb [14]–[19], screened Coulomb [20], logarithmic [21] and dipole [22,23] interaction between particles, the orientational melting (breaking the orientational order between the shells) precedes melting inside the shells. Namely, the reorientations of shells (jump rotational diffusion) or (with increasing temperature) free relative rotation of shells take place before shell structure breaking. This phenomenon is referred to as orientational melting. Moreover, the study of free relative rotation of shells may be interesting for nanomechanics [?].

The van der Waals interaction between atoms of neighbor shells in carbon nanoparticles is considerably weaker than chemical bonds between atoms inside the shell. So it is natural that these nanoparticles are possible candidates for orientational melting [5]. The possibility of orientational melting of long two-shell carbon nanotube was discussed [25]. The orientational melting in carbon nanotube bundle was also theoretically studied [26].

In the present paper the zero temperature energetic characteristics of two-shell carbon nanoparticle  $C_{60}@C_{240}$  are calculated. The values obtained for barriers of relative rotations of shells are small enough for free rotation of shells to take place at room temperature. The orientational melting of this nanoparticle is studied here by molecular dynamics technique. The definition of orientational melting temperature is proposed. The corresponding temperature for nanoparticle  $C_{60}@C_{240}$  is calculated

## II. SIMULATION DETAILS

The following reasons have determined our choice of nanoparticle shells. The TEM images show that the inner shell of carbon nanoparticle can have a size that is close to that of fullerene  $C_{60}$  [27,28]. The fullerene  $C_{60}$  with  $I_h$  symmetry is the smallest fullerene without adjacent pentagons in its structure. Fullerenes smaller than  $C_{60}$  can not be directly extracted by the use of any solvent from soot, obtained in arc discharge (see, e. g., Refc. [29,30]). To explain this fact it was proposed that atoms of fullerenes which belong to two adjacent pentagons can have chemical bonds with neighbor fullerenes in soot [32]. For example, chemical bonds between all neighbor fullerenes are present in solid  $C_{36}$  [34]. Therefore we consider  $C_{60}$  as the smallest inner shell where the absence of chemical bonds between shells is very probable (it is a necessary condition for existence of relative rotation of shells). The single and double bonds lengths of  $C_{60}$  used are 1.391 Å and 1.455 Å, respectively [35]. We accept the fullerene  $C_{240}$  with  $I_h$  symmetry

---

\*Corresponding author. Fax: +7-095-334-0886; e-mail: lozovik@isan.troitsk.ru

as outer shell of nanoparticle. This model gives the distance between shells in agreement with experiment [28] being close to the distance between graphite planes. Besides, fullerene  $C_{240}$  with  $I_h$  symmetry have greater binding energy than fullerenes  $C_{240}$  with other structures [7]. Several sets of geometric parameters corresponding to different shapes of fullerene  $C_{240}$  obtained by *ab initio* calculations of minima of binding energy [5,8,9] are used. Different shell shapes  $B$ ,  $C$ ,  $D$  and  $E$  were found by optimization of all independent geometric parameters of fullerene  $C_{240}$  with  $I_h$  symmetry. The  $B$  and  $D$  shapes corresponding to global and local minima found by York *et al* [8] that are close to sphere and truncated icosahedron, respectively. Shape  $E$  corresponds to the single minimum found by Osawa [5]. It is intermediate between shapes  $B$  and  $D$ . Shape  $C$  is rather close to shape  $E$ . It corresponds to the minimum found by Scuseria [9]. The shape  $A$  is obtained by optimization of fewer of independent geometric parameters so that all atoms of this shape are arranged on the sphere [8].

We describe the interaction between atoms of neighbor shells by Lennard-Jones potential  $U = 4\epsilon((\sigma/r)^{12} - (\sigma/r)^6)$  with parameters  $\epsilon = 28$  K and  $\sigma = 3.4$  Å. These parameters were used for the simulation of solid  $C_{60}$  [36]. The interaction between atoms inside shells are described by Born potential:

$$U = \frac{\alpha - \beta}{2} \sum_{i,j=1}^{60} \left( \frac{(\mathbf{u}_i - \mathbf{u}_j) \mathbf{r}_{ij}}{|\mathbf{r}_{ij}|} \right)^2 + \frac{\beta}{2} \sum_{i,j=1}^{60} (\mathbf{u}_i - \mathbf{u}_j)^2 \quad (1)$$

where  $\mathbf{u}_i$ ,  $\mathbf{u}_j$  are displacements of atoms from equilibrium positions,  $\mathbf{r}_{ij}$  are distances between atoms. We take  $\alpha = 1.14 \cdot 10^3$  N/m and  $\beta = 1.24 \cdot 10^2$  N/m. Born potential with these values of force constants gives an adequate internal vibrational spectrum of  $C_{60}$  [37]. Born potential is correct only near the bottom of potential well. Nevertheless we believe that this potential is adequate for our simulation because we use it at temperatures that are one-two order of magnitude less than the temperature of fullerene destruction.

We studied the orientational melting of nanoparticle  $C_{60}@C_{240}$  with shape  $D$  of  $C_{240}$  by molecular dynamics technique. The simulations are performed in microcanonical ensemble. The equations of motion were integrated using the leap frog algorithm. We used the integration step  $\tau = 6.1 \cdot 10^{-16}$  s (about one hundred steps for period of atoms vibration inside shells). Initially the system has been brought to the equilibrium during 300-500 ps that is about 30-50 librations of shells. The average fluctuations of the total energy and temperature of the system fall and flatten out during this period. Then the system was studied during 100 ps. The average fluctuations of the total energy of the system were within 0.3 % and the average fluctuations of temperature were within 1.3 %. The angular velocities of shells change rather slowly to average the properties of system over the different directions of angular velocities during one computer experiment. Therefore all investigated quantities were averaged over 34-46 different realizations of the systems at the same temperature but with different random angular velocities of shells corresponding to their distribution at temperature studied.

### III. RESULTS AND DISCUSSION

#### A. Ground state energetics

The global and local minima of total nanoparticle energy are found by optimization of three angles of their *relative* orientation. The total nanoparticle energy includes the energy of interaction between shells and the energy of shell deformation. We describe the relative orientations corresponding to minima of total energy in terms of three angles  $\alpha_z$ ,  $\alpha_y$  and  $\alpha_x$  of subsequent rotations of first shell around axes OZ, OY and OX of coordinate system. The centers of both shells coincide with the center of coordinate system. The angles  $\alpha_z$ ,  $\alpha_y$  and  $\alpha_x$  were measured from the initial orientation shown on Fig. 1. Due to the high  $I_h$  symmetry of shells the number of any equivalent minima (global or local) is 60. Such equivalent minima correspond to different relative orientations of shells. The energies of interaction between shells and angles of one of the orientations corresponding to global and local minima of total energy of nanoparticle are listed in Table 1.

The energies of interaction between shells calculated here are slightly less than 16.9 [10], 18.57 [11] and 20.3 [10] meV/atom obtained using another representations of van der Waals interaction and are about three times less than estimation 65.3 meV/atom for graphite [38]. Note, that the energy of total interaction between shells is not maximal for perfect sphere in comparison with other shapes of  $C_{240}$  contrary to the assumption of Lu and Yang [11].

We observed that the angles of orientations corresponding to global and local minima are determined by the shape of second shell. For shapes  $C$ ,  $D$  and  $E$  of  $C_{240}$  the initial relative orientation of shells (where symmetry axis of shells coincide) corresponds to global minima of total nanoparticle energy (note, that all these shapes of  $C_{240}$  are close to the truncated icosahedron). Several global minima for shape  $D$  are shown on Fig. 2a. One type of local minima is found for these shapes of  $C_{240}$ . For the shape  $B$  (which is close to sphere) orientations with coinciding symmetry axes

correspond only to local minima (see Fig 2b). No minima correspond to such orientations for the "spherical" shape A. For the "spherical" shape of  $C_{240}$  two types of local minima are found. The differences  $\Delta E_{loc}$  in total nanoparticle energies between global and local minima are very small and also determined by the shape of second shell (see Table 2). The differences  $\Delta E_{loc}$  decrease with decreasing the average deviation  $\langle \Delta R_{i2} \rangle = \langle |R_{i2} - \langle R_{i2} \rangle| \rangle$  of second shell from perfect sphere, where  $R_{i2}$  is the distance between an atom of second shell and the center of nanoparticle. Thus the differences  $\Delta E_{loc}$  are small for the "spherical" shape A and close to sphere shape B. The differences  $\Delta E_{loc}$  also decrease when the average distance between shells  $h = \langle R_{i2} \rangle - \langle R_{i1} \rangle$  approaches the distance  $r_{min}$  corresponding to the minimum in pair interatomic potential. This fact can be explained as follows: the smaller is the difference between  $h$  and  $r_{min}$  the lesser part of distances  $d_{12}$  between two atoms of neighbor shells corresponds to steeply rising interatomic potential well. Consequently, the change of distances  $d_{12}$  during relative rotation of shells causes the less change of interaction energy between shells.

The calculated energies of shell deformation are presented in Table 2. The influence of shell deformation on the barriers of relative rotation of shells is studied as an example for barriers  $B_5$  of shell rotation around fivefold axes. (Barriers  $B_5$  were calculated for the relative orientation where symmetry axes of shells have the same directions). Comparison of barriers  $B_5$  calculated with and without shell deformation gives a difference less than 1 % for all five shapes of  $C_{240}$  investigated here. (Note that the barrier  $B_5$  calculated here for the shape E of  $C_{240}$  is 12 % less than that obtained by Osawa [5] who used the tandem of molecular orbital and molecular mechanics calculations). Therefore, the shell deformations are disregarded here in calculation of barriers of relative rotation of shells, i.e. lengths of bonds and angles between bonds inside shells are supposed to be fixed during intershell rotation. Note that an opposite situation take place, e.g. for clusters with logarithmic interaction between particles [21]. In this case, the interparticle interactions inside shell and between shells are the same and, therefore, the considering of shells deformation is necessary in calculation of barriers for rotation. The relative displacement of the centers of symmetry of shells causes an increase in intershell interaction energy. Therefore, the common center of symmetry of both shells is also supposed to be fixed during rotation.

The barriers of relative rotation of shells in the nanoparticles under consideration are calculated for relative orientations corresponding to global minima of total nanoparticle energies. It is found that the values of barriers obtained for rotation are *surprisingly small* (see Table 2). Moreover, these barriers are only several times greater than barriers  $B_a$  in dependencies of interaction energy between *only one atom* of the second shell and the whole first shell vs. angle of rotation. For example, for the nanoparticle with shape D of  $C_{240}$  the barrier for rotation around fivefold axis is 158.8 K. Simultaneously, the maximal barrier among the barriers  $B_a$  for different atoms of the second shell is 21.6 K. Detailed analysis shows that maxima of barriers  $B_a$  for individual atoms in the same shell correspond to *different* angles of rotation and so the dependence of total energy on angle of rotation is *essentially smoothed* (see Fig. 3). Magnitudes of barriers of relative shell rotation are very sensitive to the shape of  $C_{240}$  and decrease when  $\langle \Delta R_{i2} \rangle \rightarrow 0$  and  $h \rightarrow r_{min}$  (analogously to the differences  $\Delta E_{loc}$  in interaction energies between global and local minima). Note that the using of spherical shape of  $C_{240}$  leads to significant underestimation of barriers for rotation.

The radii of shells of nanoparticle  $C_{60}@C_{240}$  are very close to radii of shells of (5,5)@(10,10) two-shell carbon nanotube. It is interest that barriers for relative rotation of shells per one atom calculated here for all considered nanoparticles are order of magnitude less than appropriate barrier in (5,5)@(10,10) two-shell carbon nanotube calculated by Kwon and Tomanek [25].

## B. Molecular dynamics simulation

We have investigated by molecular dynamics technique the angular velocity autocorrelation function of shells, the spectrum of shell librations, the frequency of shell reorientations, distributions of Euler angles of relative orientations of shells, heat capacity of nanoparticle and barriers in intershell interaction energy corresponding to shell reorientation events.

The dependence of total energy on temperature is used to calculate the heat capacity of nanoparticle. In the 30 – 150 K temperature region investigated the heat capacity per one degree of freedom has no difference from the heat capacity of harmonic oscillator system within the accuracy of calculation that is less than 5 %. Only three degrees of freedom are accounted for relative orientation of shells. Therefore, as was to be expected, there is not any peculiarities in the dependency of heat capacity on temperature and the orientational melting of two-shell carbon nanoparticle has a crossover behavior.

The dependence of shells reorientation frequency  $\nu$  vs. temperature  $T$  is shown on Fig. 4. The jump orientational intershell diffusion takes place where  $kT \ll B_{ef}$ ,  $B_{ef}$  is an effective energy barrier of reorientation. We interpolate the reorientation frequency  $\nu$  for jump orientational intershell diffusion at temperatures 30 – 100 K by the Arrhenius formula (thick line on Fig. 4):

$$\nu = \Omega_0 \exp\left(-\frac{B_{ef}}{kT}\right), \quad (2)$$

where  $\Omega_0$  is a frequency multiplier. The fitting by least square technique gives  $B_{ef} = 167 \pm 22$  K and  $\Omega_0 = 540 \pm 180$  ns<sup>-1</sup>. Using a shorter temperature range  $T = 30 - 75$  K for interpolation is found to have only a slight influence on calculated parameters  $B_{ef}$  and  $\Omega_0$ . Note, that effective barrier of reorientation  $B_{ef}$  is in good agreement (within the accuracy of calculation) with the minimal  $B_{min}$  and average  $B_{av}$  barriers for rotation of shells at zero temperature. Therefore it is possible to use barriers  $B_{min}$  and  $B_{av}$  as effective barrier of reorientation to estimate the temperature of orientational melting of carbon nanotubes and nanoparticles with shell structure.

The exponential increase of reorientation frequency  $\nu$  ends at temperatures 100 – 150 and this shows the beginning of free rotation of shells. It can be shown that the reorientation frequency  $\nu$  at temperature  $kT \gg B_{ef}$  can be estimated by the expression

$$\nu = \frac{n}{2\pi} \sqrt{\frac{3kT(I_1 + I_2)}{I_1 I_2}} \quad (3)$$

where  $n$  is an average number of reorientations over the period of relative shell rotation ( $n \approx 5$ ),  $I_1$  and  $I_2$  are moments of inertia of 1-st and 2-nd shells, respectively. The dependence of reorientation frequency on temperature defined by Eq. (3) is shown on Fig. 4 by thin line.

The prominent smooth distributions of Euler angles of relative orientations of shells (Fig. 5), the disappearance of maxima in the angular velocity autocorrelation function of shells (Fig. 6) and in the spectrum of shell librations (Fig. 7) confirm that the free rotation of shells determines the thermodynamical behavior of the nanoparticle at temperatures greater than 140 .

The temperature dependence of the "experimental" barriers  $B_{re}$  in intershell interaction energy corresponding to shell reorientations events is shown on Fig. 8. The barriers  $B_{re}$  are averaged over all observed reorientation events at corresponding temperature (30–70 reorientation events for each temperature investigated from range  $T = 40 - 55$  K and 200–600 reorientation events for each temperature investigated from range  $T = 70 - 150$  K). At temperatures 30–100 K, where the jump orientational intershell diffusion takes place, barrier  $B_{re}$  is in agreement (within the accuracy of calculation) with the minimal barrier  $B_{min}$  for rotation of shells at zero temperature and with effective barrier of reorientation  $B_{ef}$ . At temperatures 100 – 150 , where free rotation of shells begins, the magnitude of "experimental" barrier  $B_{re}$  grows and the increase of this barrier  $\delta B_{re}$  runs to 50 K at temperature 154 K. The increase  $\delta B_{re}$  is greater than the dispersion  $\Delta B_{av} = 10$  K of barriers for rotation of shells at zero temperature. Consequently, the increase  $\delta B_{re}$  of the barrier can not be explained by climbing over the barrier with increasing temperature not only at their lowest point. Therefore, we believe that the increase  $\Delta B_{re}$  of the barrier is the result of shell deformation. The increase of the dispersion  $\Delta B_{re}$  of "experimental" barrier with increasing temperature (see Fig. 9) also indicates the influence of shell deformation on this barrier. Note that energy of shell deformation is three order of magnitude greater than the increase  $\delta B_{re}$  of "experimental" barrier in the result shell deformation. (The energies calculated of shell deformation  $E_d$  are in agreement with virial theorem  $E_d = kT(3N - 6)/2$ , where  $N$  is number of atoms in a shell.)

Phenomena of order breaking in the systems with finite number of particles occur as a rule at some temperature range. This leads to problems in attempting to define the temperature of order breaking (see, e.g., Ref. [39] and references herein). In the majority of cases a melting of clusters occurs with change of cluster structure. That is the system become spend time with increasing temperature not only in the ground state but also in states with the structure corresponding to other minima in potential energy of system. A mesoscopic system can fluctuate between different states separated by an energy barrier: the solid state corresponding to the ground state of the system and the liquid-like state corresponding to other minima in potential energy (see, e.g., Refc. [?]). To characterize such a system at its melting the quantity  $K(T) = \gamma_l/\gamma_s$  was introduced [40], where  $\gamma_l$  and  $\gamma_s$  are the probabilities that the system is at the temperature  $T$  in liquid-like state and solid state, respectively. In this case the temperature  $T_c$  corresponding to  $K(T_c) = 1$  may be considered as melting temperature.

The situation is different for the considered nanoparticle  $C_{60}@C_{240}$ . The reorientations of shells are transitions between states corresponding to *equivalent* minima of potential energy. That is the structure of system does not change during orientational melting. To characterizes the melting of such systems, where diffusion occurs during the melting but the structure of the system does not change, we introduce the quantity  $K(T) = \nu_t/\omega_t$ , where  $\nu_t$  is the frequency of transitions between equivalent minima of potential energy and  $\omega_t$  is the frequency of such oscillation wherein movement of particles directed along the path of transition. For considered systems we propose to define the temperature  $T_c$  corresponding to  $K(T_c) = 1$  as the melting temperature. In this case a half of appropriate oscillations follows by transition to equivalent minima. Note, that proposed definition corresponds to a temperature of short

order breaking and has no analogy with phase transitions in macroscopic systems (contrary to above definition for the systems with transitions between inequivalent minima).

The appropriate quantity characterizing the orientational melting of nanoparticle  $C_{60}@C_{240}$  is  $K_o(T) = \nu/\omega$ , where  $\nu$  is the shell reorientation frequency and  $\omega$  is the frequency of relative librations of shells. The equality  $K_o = 1$  implies that a half of relative librations of shells begins in one minimum in dependence of potential energy of nanoparticle on angles of relative shell orientation and ends in neighbor equivalent minima. The estimation with the help of simulation performed gives the temperature  $T_c$  of orientational melting for nanoparticle  $C_{60}@C_{240}$  with shape  $D$  of the second shell  $T_c \approx 60$  K ( $T_c$  corresponds to  $K_o(T_c) = 1$ ). Here the frequency of relative librations of shells is determined from the maximum in the spectrum of shell librations (see Fig. 7).

As we have shown, the barriers for rotation are very sensitive to the shape of shells. Therefore, the realization of possible orientational melting in many-shell nanoparticles is determined by their shape. The nanoparticles obtained in arc discharge are faceted in shape [3,4]. However, their shape changes to almost spherical one when they are subjected to very strong electron irradiation in a high-resolution electron microscope [28,38,41]. Accurate *ab initio* calculation of geometric parameters of large shells is necessary for performance of theoretical studies of possible orientational melting of many-shell nanoparticles. Nevertheless, the theory does not provide accurate coordinates. Some works predict that many-shell nanoparticles are faceted [7,10], some that they are spherical [11,13], and some the transition from faceted to spherical shape for shells containing more than 3500 atoms [42]. The calculations have also shown that the faceted nanoparticles transform to spherical under high temperature [10,12]. Therefore, the barriers for rotation may *decrease* with *increasing* of temperature due to change of shell structure. Thus it is found that temperature of orientational melting  $T_c \approx 60$  K for two-shell carbon nanoparticle is at least one order of magnitude less than the temperature of total melting. Analogously orientational melting can occur also in many-shell nanoparticles and short many shell nanotubes [24].

The carbon nanoparticles with shell structure are not the single example of different types of atom interaction inside shell and between shells. A two-shell spherical nanoparticle from  $MoS_2$  was produced [13]. We believe that orientational melting can also take place in nanoparticles from this and analogous sandwich materials ( $MX_2$ ,  $M = Mo, W$ ,  $X = S, Se$ ).

The orientational melting in a single nanoparticle may be revealed by IR or Raman study of the temperature dependence of width of spectral lines. The last must have Arrhenius-like contribution in reorientational phase (analogously to the behavior in plastic crystals, see, e.g., Ref. [43] and references herein). Moreover, this study can give the estimation of reorientational barriers. Besides, NMR line narrowing can be observed in reorientational phase.

## ACKNOWLEDGEMENTS

This work was supported by grants from Russian Foundation of Basic Researches, Programs "Fullerenes and Atomic Clusters" and "Surface and Atomic Structures".

- 
- [1] H.W. Kroto, J.R. Heath, S.C. O'Brien, R.F. Curl, R.E. Smalley, Nature 318 (1985) 162.
  - [2] W. Kratschmer, L.D. Lamb, K. Fostiroupolos, D.R. Huffman, Nature 347 (1990) 354.
  - [3] S. Iijima, J. Crystal Growth, 50 (1980) 675.
  - [4] D. Ugarte, Chem. Phys. Lett. 198 (1992) 596.
  - [5] M. Yoshida, E. Osawa, Ful. Sc. & Tech. 1 (1993) 54.
  - [6] D. Tomanek, W. Zhang, E. Krastev, Phys. Rev. B 48 (1993) 15461.
  - [7] A. Maiti, C.J. Brabec, J. Bernhole, Phys. Rev. Lett. 70 (1993) 3023.
  - [8] D. York, J.P. Lu, W. Yang, Phys. Rev. B 49 (1994) 8526.
  - [9] G.E. Scuseria, Chem. Phys. Lett. 243 (1995) 193.
  - [10] A. Maiti, C.J. Brabec, J. Bernhole, Mod. Phys. Lett. B 7 (1993) 1883.
  - [11] J.P. Lu, W. Yang, Phys. Rev. B 49 (1994) 11421.
  - [12] A. Maiti, C.J. Brabec, J. Bernhole, Chem. Phys. Lett. 219 (1994) 473.
  - [13] D.J. Srolovita, S.A. Safran, M. Homyonfer, R. Tenne, Phys. Rev. Lett. 74 (1995) 1779.
  - [14] Yu.E. Lozovik, Usp. Fiz. Nauk (in Russian) 153 (1987) 356 [Sov. Phys. Usp. 30 (1987) 912].
  - [15] Yu.E. Lozovik, V.A. Mandelshtam, Phys. Lett. A 145 (1990) 269.

- [16] Yu.E. Lozovik, E.A. Rakoch, Phys. Lett. A 240 (1998) 311.
- [17] A.V. Filinov, M. Bonits, Yu.E. Lozovik, Phys. Rev. Lett. (in print).
- [18] V.M. Bedanov, F.M. Peeters, Phys. Rev. B 49 (1994) 2667.
- [19] F.M. Peeters, V.M. Schweigert, V.M. Bedanov, Physica B 212 (1995) 237.
- [20] G.E. Astrakharchik, A.I. Belousov, Yu.E. Lozovik, Phys. Lett. A 258 (1999) 123.
- [21] Yu.E. Lozovik, E.A. Rakoch, Phys. Rev. B 57 (1998) 1214.
- [22] Yu.E. Lozovik, E.A. Rakoch, Phys. Lett. A 235 (1997) 55.
- [23] A.I. Belousov, Yu.E. Lozovik, Eur. Phys. D 8 (2000) 251.
- [24] Yu.E. Lozovik, to be published.
- [25] Y.K. Kwon, D. Tomanek, Phys. Rev. B 58 (1998) R16001.
- [26] Y.K. Kwon, D. Tomanek, Phys. Rev. Lett. 84 (2000) 1483.
- [27] S. Iijima, J. Phys. Chem. 91 (1987) 3466.
- [28] D. Ugarte, Nature 359 (1992) 707.
- [29] D.M. Parker, P. Wurz, K. Chatterjee, K.R.E. Lykke, J.E. Hunt, M.J. Pellin, J.C. Hemminger, D.M. Gruen, L.M. Stock, J. Am. Chem. Soc. 113 (1991) 7499.
- [30] Y. Chai, T. Guo, C. Jin, R.E. Haufler, L.P.F. Chibante, J. Fure, L. Wang, J.M. Alford, R.E. Smalley, J. Phys. Chem. 95 (1991) 7564.
- [31] Yu.E. Lozovik, A.M. Popov, Phys. Low-Dim. Str. 6 (1994) 33.
- [32] Yu.E. Lozovik, A.M. Popov, Physics Uspekhi 40 (1997) 717.
- [33] Yu.E. Lozovik, A.M. Popov, in Physics of Clusters, eds. G.N.Chuev and V.D.Lakhno (World Scientific Publishing, Singapore, 1998) 1-55.
- [34] C. Pishoti, J. Yarger, A. Zetti, Nature 395 (1998) 771.
- [35] W.I.F. David, R.M. Ibberson, J.C. Matthewman, K. Prassides, T.J.S. Dennis, J.P. Hare, H.W. Kroto, R. Taylor, D.R.M. Walton, Nature 353 (1991) 147.
- [36] A. Cheng, M.L. Klein, J. Phys. Chem. 95 (1991) 6750.
- [37] Q. Jiang, H. Xia, Z. Zhang, D. Tian, Chem. Phys. Lett. 191 (1991) 197.
- [38] D. Ugarte, Europhys. Lett. 22 (1993) 45.
- [39] P.Borrmann, O. Mulken, J. Hurting, Phys. Rev. Lett., 84 (2000) 3511.
- [40] J. Jellinek, T.L. Beck, R.S. Berry, J. Chem. Phys., 84 (1986) 2783.
- [41] D. Ugarte, Chem. Phys. Lett. 207 (1993) 473.
- [42] A. Perez-Garrido, Phys. Rev. B 62 (2000) 6979.
- [43] G.N. Zhizhin, Yu.E. Lozovik, M.A. Moskalova, A. Usmanov, Soviet Physics-Doklady 15 (1970) 36.

Table 1.

The energies  $E_{int}$  of interaction between nanoparticle shells and one of the relative orientations of shells corresponding to the global and local minima of total nanoparticle energy;  $\alpha_z$ ,  $\alpha_y$  and  $\alpha_x$  are the angles of subsequent rotations of inner shell from initial orientation around axes OZ, OY and OX, respectively.

Shape	$E_{int}$ , (meV/atom)	$\alpha_z$ (in radians)	$\alpha_y$ (in radians)	$\alpha_x$ (in radians)
<i>A</i>	15.034	0.0819	0.1452	0.0540
<i>A</i>	15.033	0.2495	0.8128	-0.0081
<i>A</i>	15.032	0.6283	0.4634	0.0
<i>B</i>	15.124	0.6283	0.4634	0.0
<i>B</i>	15.101	0.0	0.0	0.0
<i>C</i>	15.180	0.0	0.0	0.0
<i>C</i>	15.098	0.6283	0.4634	0.0
<i>D</i>	13.819	0.0	0.0	0.0
<i>D</i>	13.777	0.6283	0.4634	0.0
<i>E</i>	15.166	0.0	0.0	0.0
<i>E</i>	15.061	0.6283	0.4634	0.0

Table 2.

The characteristics of second shell shape: the average deviation of second shell from perfect sphere  $\langle \Delta R_{i2} \rangle$  and the difference between average intershell distance  $h$  and the distance  $r_{min}$  corresponding to the minimum in pair interparticle potential  $l = h - r_{min}$ ; the differences  $\Delta E_{loc}$  in total energies of nanoparticle between global and local minima; the minimal and average barriers for rotation  $B_{min}$ ,  $B_{av} \pm \Delta B_{av}$ , respectively, where the barrier  $B_{av}$  is averaged over all directions of rotation axis and  $\Delta B_{av}$  is its dispersion; the average energies of shell deformation  $E_{d1} \pm \Delta E_{d1}$  and  $E_{d2} \pm \Delta E_{d2}$  for first and second shells, respectively, where the energies  $E_{d1}$  and  $E_{d2}$  are averaged over all relative orientations of shells and  $\Delta E_{d1}$  and  $\Delta E_{d2}$  are their dispersions.

Shape	$\langle \Delta R_{i2} \rangle$ (Å)	$l$ (Å)	$\Delta E_{loc}$ (°K)	$B_{min}$ (°K)	$B_{av} \pm \Delta B_{av}$ (°K)	$E_{d1} \pm \Delta E_{d1}$ (°K)	$E_{d2} \pm \Delta E_{d2}$ (°K)
<i>A</i>	-0.245	0.0	3.2; 5.5	19.0	$20.5 \pm 0.8$	$2.09 \pm 0.02$	$34.56 \pm 0.12$
<i>B</i>	-0.258	0.057	76.7	82.9	$122.1 \pm 12.1$	$1.62 \pm 0.07$	$29.98 \pm 0.50$
<i>C</i>	-0.289	0.152	287.4	349.3	$363.1 \pm 8.8$	$2.17 \pm 0.26$	$18.19 \pm 0.42$
<i>D</i>	-0.119	0.244	144.4	160.3	$177.3 \pm 9.6$	$3.75 \pm 0.20$	$34.40 \pm 0.55$
<i>E</i>	-0.299	0.147	368.3	441.2	$459.9 \pm 12.9$	$4.58 \pm 0.44$	$13.78 \pm 0.38$



### Captions for illustrations.

**Fig. 1.** The fragments of two shells (shape  $D$  of second shell) at their initial orientations. OX, OY and OZ are axes of coordinate system. One fivefold axis of each shell is aligned with the axis OZ. One of the closest to axis OZ atoms of first and second shells (shown by black circles) lie in plane OXZ. This fixes the orientation of axes OX and OY.

**Fig. 2.** The dependencies of binding energies for interaction between shells of nanoparticle on their relative orientation.  $\alpha_z$  and  $\alpha_y$  are the angles of subsequent rotations of inner shell from initial orientation around axes Z and Y respectively. The angle of rotation around axis X is fixed equal to zero. a) shape D of second shell; b) shape B of second shell;

**Fig. 3.** Interaction energies between first shell of nanoparticle and groups of atoms of second shell with shape  $D$  vs. angle  $\alpha_z$  of rotation of inner shell from initial orientation around axis Z. An each group include all atoms with the same dependencies of interaction energy  $E_a$  between this atom and the first shell on angle of rotation. The curves corresponding to all 25 groups of atoms with different dependencies  $E_a$  for individual atom are shown by thin lines (23 groups from 10 atoms and 2 groups from 5 atoms). The dependence of total interaction energy between shells on angle  $\alpha_z$  is shown by bold line. All energies are measured from their minima.

**Fig. 4** The dependence of shells reorientation frequency  $\nu$  on temperature  $T$  in Kelvin degrees. The interpolation by the Arrhenius formula at  $kT < B_{re}$  is shown by thick line. The estimation at  $kT > B_{re}$  is shown by thin line.

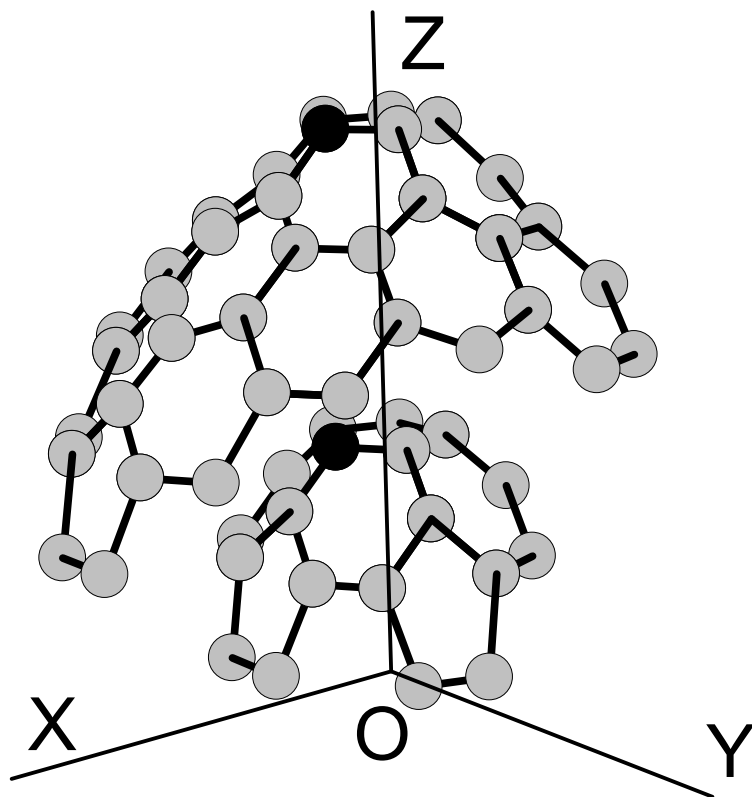
**Fig. 5** The distributions of Euler angles  $\theta$ ,  $\psi$  and  $\phi$  of relative orientations of shells at temperatures 21 K, 36 K and 140 K are shown by dotted lines, thin lines and thick lines respectively; a) the distribution of angle  $\phi$ ; b) the distribution of angle  $\theta$ ; c) the distribution of angle  $\psi$ .

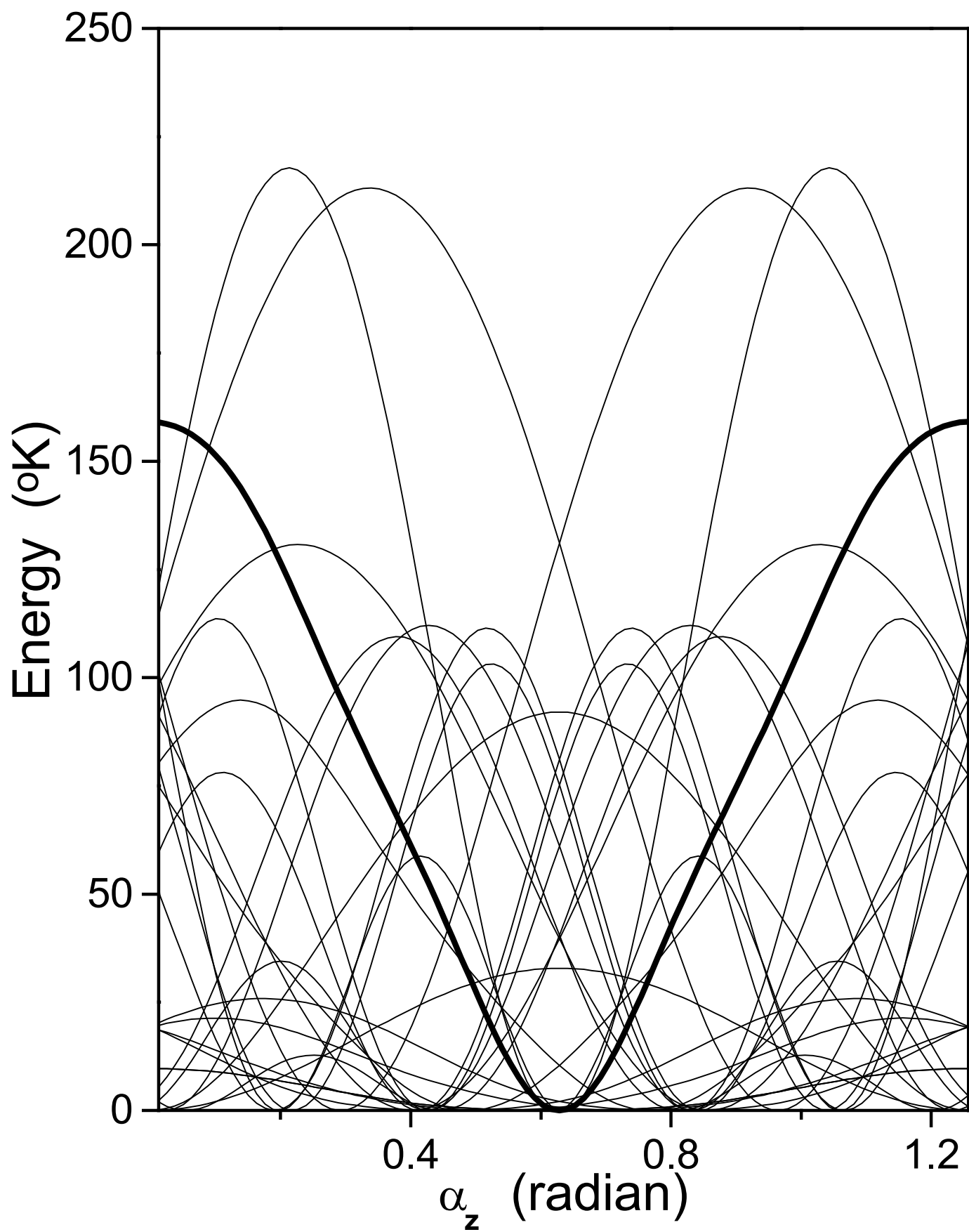
**Fig. 6** The angular velocity of autocorrelation function of the first shell at temperatures 21 K, 36 K and 140 K are shown by dotted lines, thin lines and thick lines respectively.

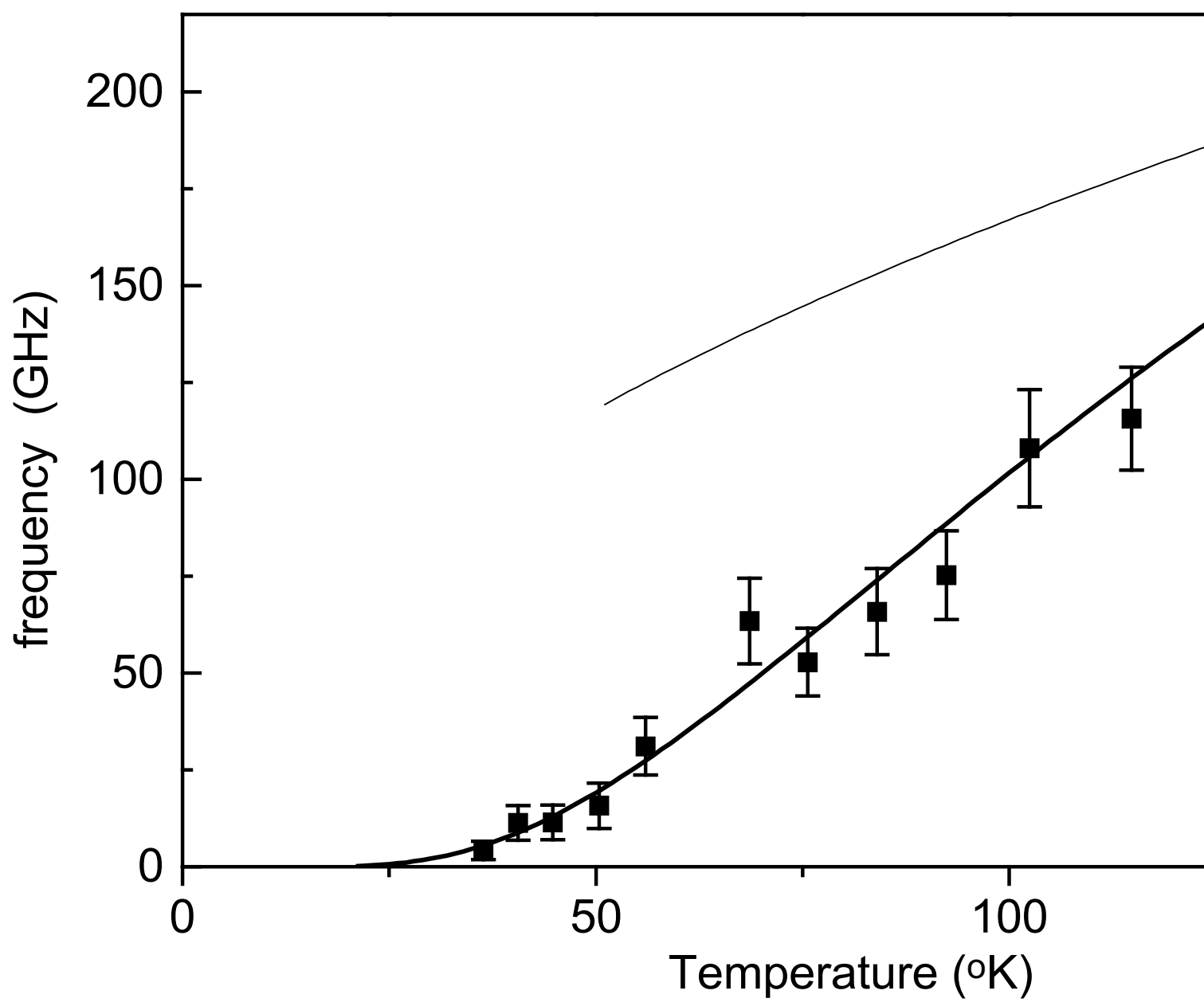
**Fig. 7** The spectrum of shell librations at temperatures 21 K, 36 K and 140 K are shown by dotted lines, thin lines and thick lines respectively.

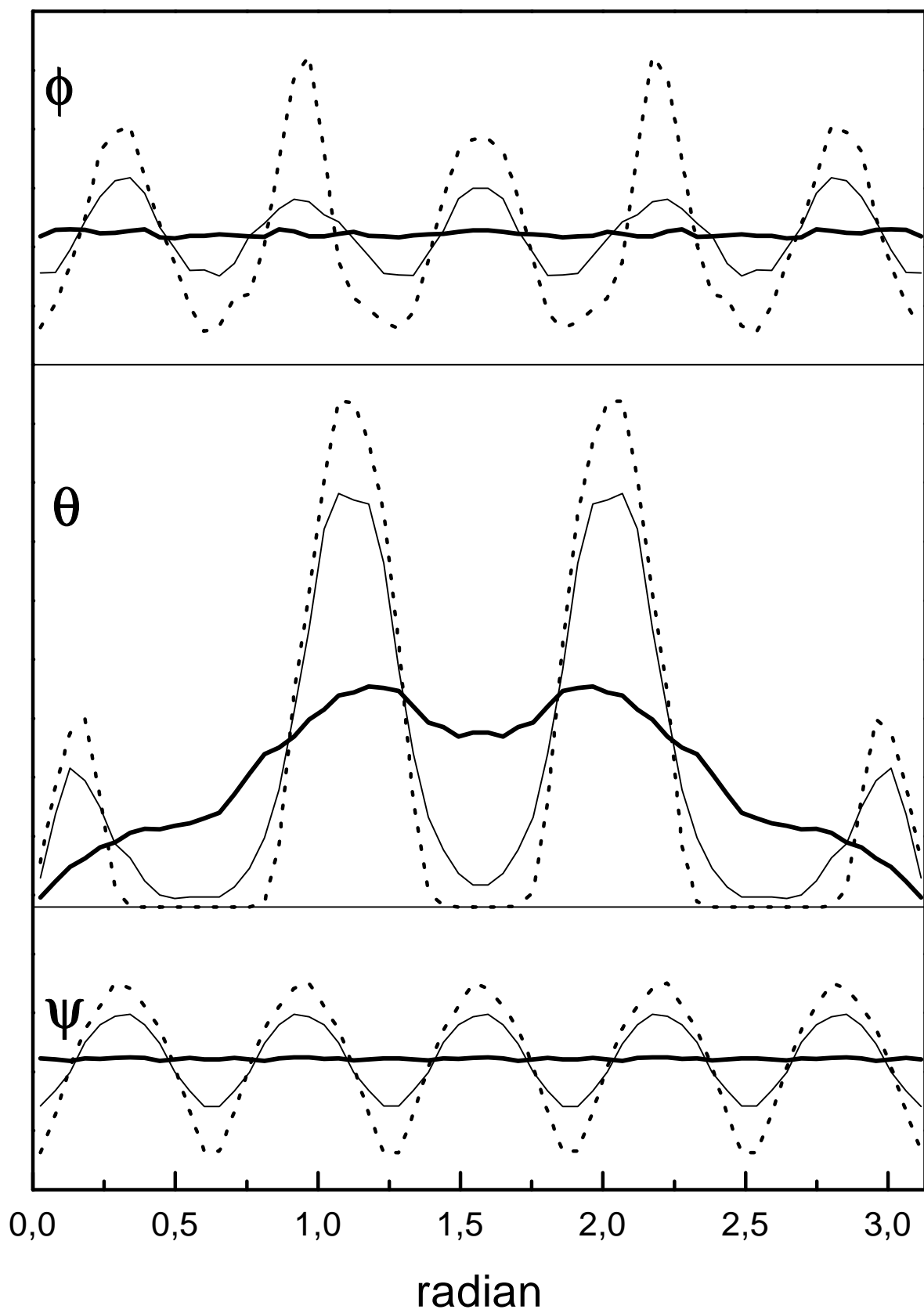
**Fig. 8** The dependence of the "experimental" barriers  $B_{re}$  in intershell interaction energy on temperature  $T$ .

**Fig. 9** The dependence of the dispersion  $\Delta B_{re}$  of barriers in intershell interaction energy on temperature  $T$ .









angular velocity autocorrelation function

